Understanding Cu sintering and its role on corrosion behaviour for high-temperature microelectronic application

Juan Ignacio Ahuir-Torres
School of Engineering, Liverpool John Moores University, Liverpool L3 3AF, UK
j.i.ahuirtorres@ljmu.ac.uk

Sri Krishna Bhogaraju
Institute of Innovative Mobility, Technische Hochschule Ingolstadt, 85049 Ingolstadt, Germany
srikrishna.bhogaraju@thi.de

Geoff West
WMG, The University of Warwick, Coventry CV4 7AL, UK
g.west@warwick.ac.uk

Gordon Elger
Institute of Innovative Mobility, Technische Hochschule Ingolstadt, 85049 Ingolstadt, Germany
gordon.elger@thi.de

Hiren R. Kotadia
School of Engineering, Liverpool John Moores University, Liverpool L3 3AF, UK
h.r.kotadia@ljmu.ac.uk

***Abstract*— There has been a significant rise in interest from academic and industry communities on copper nano- and micro-particles-based sinter pastes for harsh environment die attach. However, sintering these particles is a complex process which is affected by many parameters, such as (i) particles size, shape, and distribution, (ii) sintering temperature, pressure, environment, and (iii) organic compounds used for the paste formulation. In literature, various research groups demonstrated that sintered copper layer can achieve good electrical conductivity and high strength. In our previous research [1, 2], we explained that microscale etched flakes are also capable of shear strength >30Mpa while sintering with 10 MPa bonding pressure at 275 °C for just 1 minute with negligible paste cost (in comparison to silver paste). However, very limited knowledge exists on literature about corrosion behaviour in sintered copper interconnects. This, from experience in the industry with silver sintering has proven to be critical to applications. For examples in high power LED headlamp applications, minor exposure to residual Sulphur emerging from vulcanized rubber seals has been observed to cause corrosion in silver sintered interconnects. Therefore, corrosion and its impact on performance and reliability must be considered, especially for safety critical applications. For this reason, we have studied the relationship between copper sintered samples and corresponding corrosion behaviours and compared again to pure copper (conventionally produced). The corrosion resistance of the samples in salt water was assessed via various electrochemical analysis techniques and correlated with sintered microstructure. Sample produced better corrosion resistance when fabricated with higher density (less porosity). However, in case of the microscale copper flakes-based interconnects, a pitting behaviour was observed. The sintered copper paste samples showed to be nobler than commercial copper. In addition, copper oxide and its role in accelerating/preventing oxidation is also studied.**

Keywords—Copper sintering, high-temperature electronics, corrosion, porosity, electrochemical analysis.

I. INTRODUCTION

The increasing need for high-temperature electronics (above 175 °C) has driven various advancements in the field of die-attach bonding, ranging from the development of new high-temperature solders to silver (Ag) nanoparticle sintering [1-4]. However, these solutions tend to be relatively expensive compared to the previous solder solution based on Pb5Sn. As a result, the microelectronic industry is under significant pressure to reduce packaging costs, leading to a growing momentum in the exploration of more affordable alternatives such as copper (Cu) sintering [1, 2].

Cu has emerged as a highly promising option due to its favourable characteristics, such as its high intrinsic electrical and thermal conductivity, which is comparable to Ag but at a substantial cost advantage [5]. The industry has recognised the potential of Cu sinter pastes as a cost-effective solution to meet the requirements of high-temperature electronics while maintaining optimal performance. However, there are significant challenges to overcome [1, 2]. One major challenge is the inherent tendency of Cu to undergo oxidation, which is a spontaneous reaction that becomes more favourable with increasing temperature. Additionally, the higher melting point of Cu (1083 °C) necessitates a higher sintering temperature compared to Ag when working with particles of similar morphologies. Several solutions have been proposed to address these challenges in Cu sintering. These solutions primarily involve the use of a reducing atmosphere (such as H_2, forming gas or formic acid enriched N_2) during the sintering process or the incorporation of reducing binders in pastes [6, 7]. Other approaches include oxidation-reduction bonding processes, the utilisation of Cu core shell particles with outer layers of Ag/Sn, and the application of phosphating techniques to Cu nanoparticles. These strategies aim to mitigate the oxidation issues and optimise the sintering process for Cu, ensuring improved performance and reliability in high-temperature electronics applications. However, some of these solutions also negate the cost advantage of Cu over Ag and pose challenges towards scaling up production. Also, producing Cu nanoparticle is proven expensive and not eco-friendly.

In order to overcome the challenges associated with Cu nanoparticles, our recent development [1, 2] has been made in the form of a copper flakes-based approach. This alternative has demonstrated comprehensive advantages over existing Cu nanoparticle solutions while maintaining a negligible cost. The focus of this research is to investigate the corrosion behaviour of the Cu sintered interconnects. In this paper, a thorough examination of the microstructure has been conducted using advanced characterisation techniques,

accompanied by detailed electrochemical analyses. By correlating these results, the significance of porosity in the sintered microstructure is explained. The objective of this study is to provide a better understanding of the role of porosity on the corrosion behaviour and to identify strategies for further improvement in performance.

II. Experimental Methodology

A. Materials and sample preparation

Copper pastes were formulated by blending specially designed surface-enhanced microscale copper flakes with an organic binder using a planetary rotary mixer. The mixing sequence involved 4 minutes at 1000 rpm, followed by 5 minutes at 500 rpm. Both types of microscale particles had a flake-like morphology. Notably, particles in Paste 1 exhibited slightly greater thickness than those in Paste 2. These pastes demonstrated extended stencil life, no bleed-out during sintering, stability at room temperature, and excellent printability.

The study involved testing two distinct pastes: Paste 1 and Paste 2, both of which employed the same organic binder combination. Notably, Paste 2 contained 17 wt.% less organic content than Paste 1. Additionally, the particles in Paste 1 underwent a surface enhancement process three times less intensive than those in Paste 2.

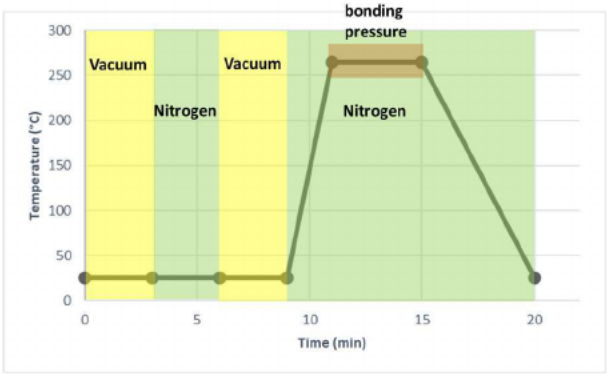

Fig. 1 Sintering profile as performed on the Budatec SP300 sinter press.

Fig. 2 Budatec SP300 sinter press used for copper sintering.

The pastes were manually printed with a 150 µm stencil onto a stainless-steel substrate. Stripes with 5 mm x 50 mm were printed. The oriented traces were pre-dried at 100°C for 5 min in air in a standard convection oven. Sintering was performed using a Budatec SP300 sinter press at 275°C for 5min with 25 MPa bonding pressure under N_2 atmosphere. Two vacuum steps to 10 mbar were executed before introducing N_2 into the sintering chamber. The resulting stripes were measured to have an average thickness of 50 ± 4 µm for Paste 1 and 72 ± 7 µm for Paste 2 sinter pastes. The thermal conductivity of the samples as measured by the LaTIMA equipment from Berliner Nanotest and Design GmbH [3], resulted in a thermal conductivity of 197±26 W/mK and 205±27 W/mK and an electrical conductivity of 20.43 ± 3.24 and 20.45 ± 1.76 MS/m for Paste 1 and Paste 2 respectively. Measurements were performed and averaged across 3 stripes for each paste.

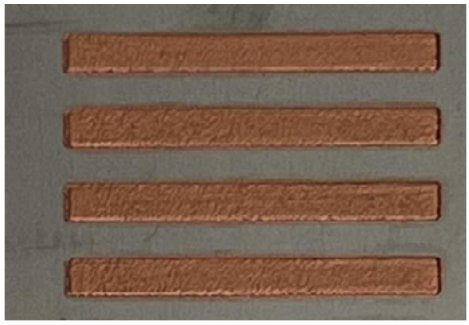

Fig. 3 Optical image of the printed Copper stripe.

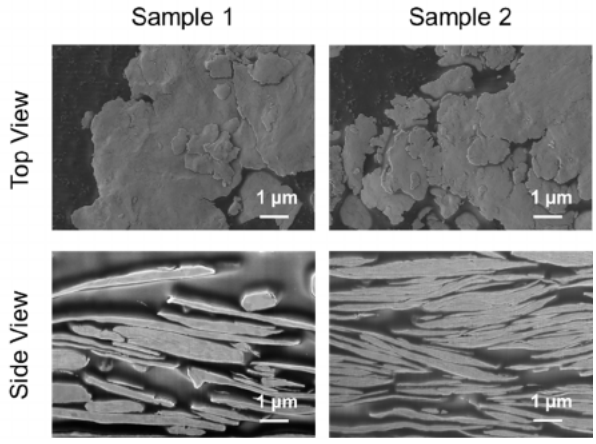

Fig. 4 SEM microstructure of the original surface-enhanced flakes of sample 1 (used for Paste 1) and sample 2 (used for Paste 2) shown from top and side views.

B. Electrochemical analyses

All electrochemical analyses were carried out with a three-electrode cell formed of a reference, counter and working electrode where reference electrode was silver/silver chloride in 3 M KCl (Ag/AgCl 3M KCl), platinum wire of 0.7 mm diameter was counter electrode the sample was the working electrode. Prior the electrochemical testing, the samples were polished at P1200 abrasive grit supplied by Struer. The samples were moreover cleaned with the next subsequent steps; firstly, the samples were cleaned with commercial detergent and fresh water, then soaked with distilled water, sprayed with isopropanol and dried with drier. The samples were let 48 hours before the electrochemical analyses to permit the native passive film generation. RS supplied the isopropanol. The electrochemical testing was conducted using a potentio/galvanostat (Interface1010E). Gamry Framework Version 7.8.4 software was employed to set the

potentio/galvanostat parameter for each electrochemical trail. Gamry Echem Analyst software was used to evaluate the electrochemical test outputs. The potentio/galvanostat and software were provided by Gamry Instruments Inc. Two electrochemical tests were performed (i) asymmetric electrochemical noise (AEN) and (ii) potentiodynamic polarisation curve (PPC). The harsh environment was 0.6 M NaCl where the salt was supplied by Merck-Sigma-Aldrich. Total time and acquisition time were 7200 seconds and 0.05 s, respectively for AEN. The potential rate initial and end potential were 0.167 mVs^{-1}, -0.3 V from open circuit potential and 2 V from reference electrode potential, correlatively for PPC. The open circuit potential was at 7200 seconds of immersion in 0.6 M NaCl. Two limit current densities were employed in PPC, being 2.5 10^{-4} Acm^{-2} and 1.0 10^{-2} Acm^{-2} for commercial copper and sintered copper ink, respectively.

C. Microstructural analysis

For microstructure analysis, the samples were prepared using a combination of mechanical grinding, polishing, and, in some cases, ion-beam milling processes. The as-received, sintered stripes were then examined using Scanning Electron Microscope (SEM) coupled with energy-dispersive X-ray spectroscopy (EDS). Additionally, the samples subjected to corrosion analysis were analysed using SEM and FIB to reveal the oxide layer on the sintered samples. The quantitatively analyses of porosity performed using open-source ImageJ software.

III. Results and Discussion

A. Microstructure analysis of Cu flake and sintered sample

Fig. 4 illustrates the SEM analysis of the as-received surface-enhanced copper flakes. The top view of the two different flakes used in this study shows no noticeable difference. However, the cross-section of the flakes revealed a clear distinction between the two samples, with flakes in sample 1 (used for the Paste 1) being thicker than those in sample 2 (used for the Paste 2). The preparation of both flakes differs significantly, with sample 2 undergoing additional enhancement processes compared to sample 1.

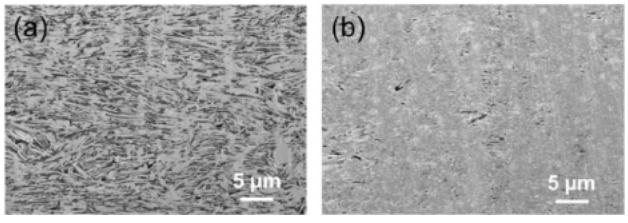

Fig. 5 SEM microstructure of the sintered samples: (a) Sample 1 (using Paste 1) and (b) Sample 2 (using Paste 2), highlighting differences in porosity volume, size, and distribution.

The surface-enhanced flakes were then used for creating the paste in combination with the novel organic binder. Fig. 5 displays cross sections of the sintered samples, revealing a distinctive sintering behaviour, with flakes stacking over each other and exhibiting significantly reduced porosity.

Additionally, a clear contrast in the sintered microstructure was observed between the pastes, as shown in Fig. 4. The results indicate that sample 1 (using paste 1) exhibited a much higher area percentage of porosity (~26%) compared to sample 2 (using paste 2) (~6%).

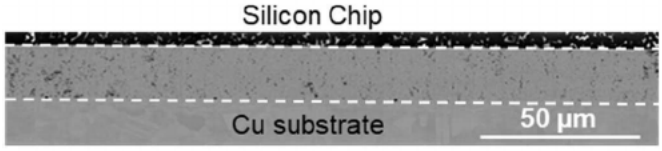

Fig. 6 SEM cross-section of silicon chip/Cu sintered (Paste 2)/Cu substrate showing a dense and homogeneous interconnect with uniformly distributed porosity.

Paste 2 was also utilised for sintering a silicon chip and Cu substrate, applying 20 MPa bonding pressure for 5 minutes at 275°C. Fig. 6 displays the cross-sectional microstructure of the sintered assembly, which demonstrates a dense and homogeneous interconnect with excellent bonding between the silicon chip and substrate. Porosity analysis of the full cross-section revealed the presence of approximately ~8 vol.% of porosity in the sintered interconnection.

This experimental investigation clearly revealed the influence of flake thickness on sintering behaviour, despite the topographical morphology remaining the same in both samples. The porosity in sample 2 is approximately 5 times lower than in sample 1, attributed to the reduction of flake thickness from ~0.5 µm to ~0.27 µm.

B. Electrochemical analysis of sintered samples

Fig. 7 illustrates AEN results over time. The potential of all samples decreased over time, as depicted in the open circuit potential (OCP) graph (Fig. 7(a)). This, indicate the oxidation of copper. The nobility (potential) of the material typically decreases due to copper oxidation by chloride ions [8]. The potentials varied among the samples, following this order: sintered copper Paste 1 > sintered copper Paste 2 > conventionally manufactured dense copper sheet. The changes in microstructure, such as grain size, impurities, and defects (e.g., porosity), significantly influence the material potentials. The copper with fine microstructure is nobler than copper with coarse microstructure because the grain boundary possesses higher corrosion potential than grain. The surfaces with larger area ratio of the boundary grain thus exhibit nobler for copper. The defects and imperfections are zones with dissimilar surface energy to matrix. This can produce activation or inactivation zones, increasing or reducing the potential of the sample [9, 10]. The sintered copper paste 2 had less porosity and may have a finer microstructure than the sintered copper paste 1. Sintered Paste 2 therefore was nobler than sintered paste 1. In the case of the higher potential of the sintered copper paste samples in comparison with commercial copper, this is owing to their finer microstructures.

In contrast to OCP results, the Zero Resistance Ammeter (ZRA) (Fig. 7(b)) results demonstrate that commercial copper and sintered copper paste-2 exhibit similar behaviours, with constant current density over time. However, in the case of Paste 1, the current density diminishes over time. This reduction can be attributed to the potential decreasing over time, as per Ohm's law [11],

suggesting that the corrosion resistance remains constant or experiences a slight reduction over time.

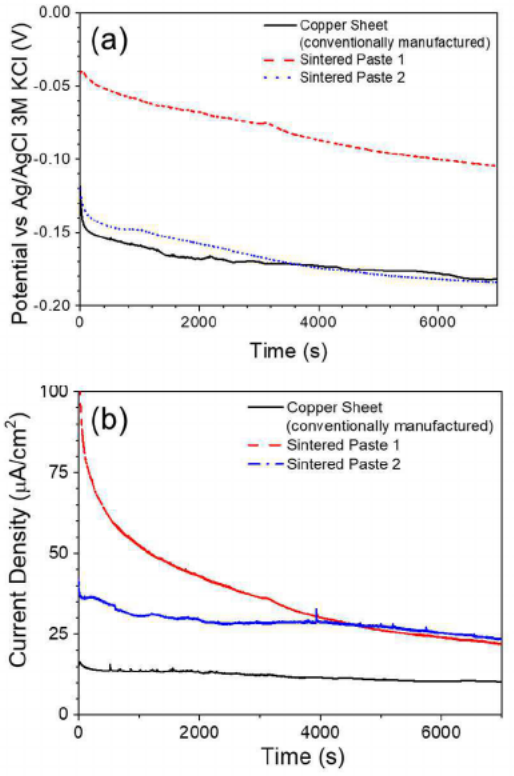

Fig. 7 AEN analysis of the commercial copper sheet, sintered copper Paste 1 and 2: (a) OCP and (b) ZRA evolution over the time for 2 hours in 0.6 M NaCl.

The second analyses preformed on the sample were PPC. The curve behaviours of the samples exhibited striking similarities, as evident from Fig. 8. The cathodic branch displayed a horizontal curve at low potential and a vertical curve at high potential. This behaviour can be attributed to the chemical evolution of hydrogen and water, wherein a portion of the PPC potential is utilized for this evolution [12]. The vertical curve signifies the diffusion control of the cathodic/reduction reactions [8].

On the other hand, the anodic branch appeared as an inclined curve, indicating a mixed control involving activation and passivation/diffusion for the oxidised/anodic reactions [8]. Notably, the PPC did not exhibit a passivation film for copper due to the rapid dissolution of the copper oxide layer caused by chloride ions [13].

The sintered copper Paste 1 exhibited the highest corrosion potential (E_{corr}), while the lowest was observed for the commercial copper. Microstructures with finer boundaries tend to generate nobler materials [9]. In the case of the sintered paste samples, the material's nobility decreases with increasing porosity [10]. These findings were consistent with the results obtained from AEN analysis.

The corrosion current density (I_{corr}) was determined by estimating the intersection of the Tafel lines. The sintered copper ink samples showed similar I_{corr} values among themselves, being higher than that of the commercial dense copper. The microstructural refinement strengthened the cathodic effect of the boundary grain on the grain [4, 14].

The presence of porosity also increased I_{corr} due to the larger contact area between the sample and the aggressive environment [9]. While these values were qualitatively similar to AEN $I_{R.M.S.}$, the quantitative values differed. This discrepancy can be attributed to the asymmetric system, which focuses the electrochemical noise on the cathodic branch [14].

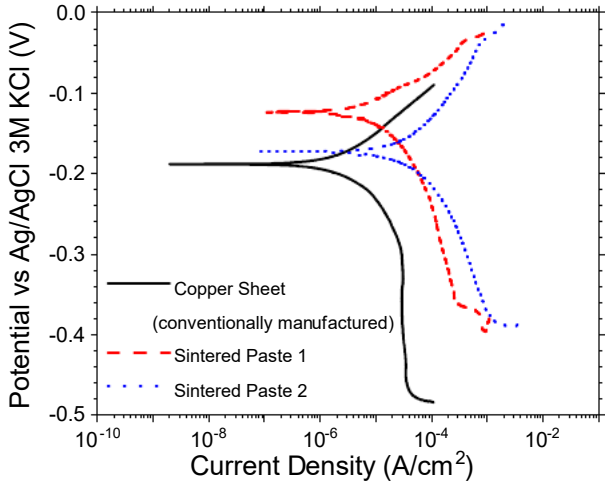

Fig. 8 PPC of the commercial copper, sintered copper Paste 1 and 2 in 0.6 M NaCl at room temperature.

C. Microstructure analysis after corrosion tests

In order to understand the distinct corrosion behaviours of the commercially manufactured dense copper sheet and sinter pastes 1 and 2, SEM analysis was carried out on the surface and cross-section of the samples after the PPC test (Fig. 9).

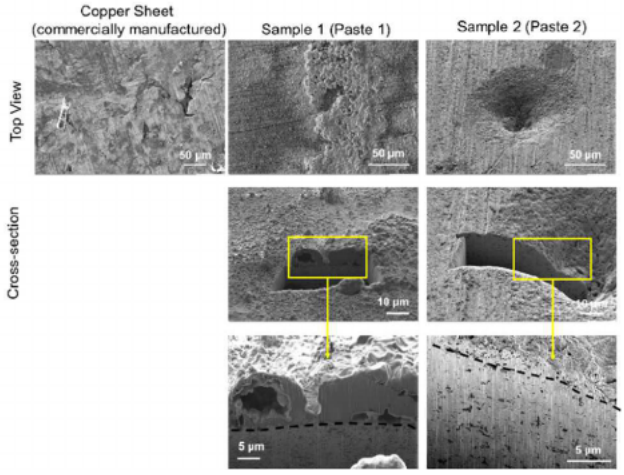

Fig. 9 SEM analysis of the samples after corrosion testing.

In the case of the commercial copper sheet, no crevice or pitting sites were observed. The only noticeable difference was observed at the grain boundaries, likely due to their increased reactivity compared to the bulk material.

Sintered Paste 1 (sample 1), which exhibits approximately 26 area. % porosity, showed pitting and oxide islands at various sites. This porosity is believed to be the cause of the pitting sites, as the native passive film is thinner on the pore, leading to localized corrosion.

On the other hand, highly sintered Paste 2 (sample 2) demonstrated better corrosion resistance, with only a few pitting sites observed. In Paste 2, not only was the porosity reduced from 26% to 6 area. %, but the size, shape, and thickness of the remaining pores were also altered. The channels between the flakes were narrowed due to flake-to-flake diffusion and grain boundary movement during sintering, promoting pore closure and resulting in smaller and fewer pits. This densification process enhanced the resistance of these compacts to pitting corrosion compared to Paste 1.

Moreover, the FIB cross-section offers additional evidence, indicating an unstable oxide layer with porosity and cracks in sample 1, contrasting with sample 2. Notably, the oxide layer is considerably thick, measuring approximately ~5 μm.

IV Conclusion

This study focuses on investigating the relationship between copper flakes, sintering, and corrosion in two different samples. The corrosion characteristics of the samples are compared against those of a commercially pure copper sheet.

The thickness of copper flakes significantly influences their sinterability due to the difference in the specific surface area of the flakes, even when the morphology of the flakes remains similar.

The variation in porosity size, shape, and distribution plays a crucial role in determining the corrosion characteristics of the sintered paste. Higher porosity levels resulted in prompting of localized pitting and the formation of a weak native passive film, leading to a higher corrosion rate compared to the densely sintered sample. The sintered copper ink samples are nobler than commercial copper because the fine microstructure.

Further investigations are required to quantify the impact of porosity size and shape on corrosion resistance and to establish a comprehensive understanding of the corrosion mechanisms over time. This knowledge will be essential for optimising sintering processes and enhancing the corrosion resistance of the materials.

Acknowledgment *(Heading 5)*

This work was partially supported by (1) Liverpool John Moore University, Faculty of Engineering and Technology (FET) Pump Prime Awards 2022/23 and (2) Copperfield (Grant number FKZ 13XP5134F) under KMU Innovative from the Federal Ministry of Education & Research, Germany. The authors would like to thank Dr. Ralf Webler from Schlenk SE for support with the SEM imaging.

References

[1] S.K. Bhogaraju, H. R. Kotadia, F. Conti, A. Mauser, T. Rubenbauer, R. Bruetting, M. Schneider-Ramelow, G. Elger, Die-Attach Bonding with Etched Micro Brass Metal Pigment Flakes for High-Power Electronics Packaging, ACS Applied Electronic Materials, 3 (2021) 4587-4603.

[2] S.K. Bhogaraju, F. Conti, H.R. Kotadia, S. Keim, U. Tetzlaff, G. Elger, Novel approach to copper sintering using surface enhanced brass micro flakes for microelectronics packaging, Journal of Alloys and Compounds, 844 (2020) 156043.

[3] D. Wakuda, M. Hatamura, K. Suganuma, Novel method for room temperature sintering of Ag nanoparticle paste in air, Chemical Physics Letters, 441 (2007) 305-308.

[4] R. Durairaj, R. Ashayer, H.R. Kotadia, N. Haria, C. Lorenz, O. Mokhtari, S.H. Mannan, Pressure free sintering of silver nanoparticles to silver substrate using weakly binding ligands, in: 2012 12th IEEE International Conference on Nanotechnology (IEEE-NANO), 2012, pp. 1-4.

[5] T.F. Chen, K.S. Siow, Comparing the mechanical and thermal-electrical properties of sintered copper (Cu) and sintered silver (Ag) joints, Journal of Alloys and Compounds, 866 (2021) 158783.

[6] S.A. Paknejad, S.H. Mannan, Review of silver nanoparticle based die attach materials for high power/temperature applications, Microelectronics Reliability, 70 (2017) 1-11.

[7] L. Wang, L. Wang, X. Meng, F.-S. Xiao, New Strategies for the Preparation of Sinter-Resistant Metal-Nanoparticle-Based Catalysts, Advanced Materials, 31 (2019) 1901905.

[8] S. Zor, Sulfathiazole as potential corrosion inhibitor for copper in 0.1 M NaCl, Protection of Metals and Physical Chemistry of Surfaces, 50 (2014) 530-537.

[9] L. Lapeire, E. Martinez Lombardia, I. De Graeve, H. Terryn, K. Verbeken, Influence of grain size on the electrochemical behavior of pure copper, Journal of Materials Science, 52 (2017) 1501-1510.

[10] D. Yang, X. Kan, P. Gao, Y. Zhao, Y. Yin, Z. Zhao, J. Sun, Influence of porosity on mechanical and corrosion properties of SLM 316L stainless steel, Applied Physics A, 128 (2021) 51.

[11] S.J. Kim, J.C. Park, S.K. Jang, Evaluation of Electrochemical Characteristics for Casted AC7AV Aluminum Alloy, Advanced Materials Research, 811 (2013) 54-60.

[12] R.G. Kelly, J.R. Scully, D. Shoesmith, R.G. Buchheit, Electrochemical Techniques in Corrosion Science and Engineering (1st ed.), CRC Press, (2002).

[13] Hamid A. Z. , Gomaa M. H., Hassan H. B., Corrosion Performance of Copper - Diamond Composites in Different Aqueous Solutions, American Journal of Electromagnetics and Applications., 4 (2016) 39-49.

[14] D.-H. Xia, S. Song, Y. Behnamian, W. Hu, Y.F. Cheng, J.-L. Luo, F. Huet, Review—Electrochemical Noise Applied in Corrosion Science: Theoretical and Mathematical Models towards Quantitative Analysis, Journal of The Electrochemical Society, 167 (2020) 081507.